Reducing Downward Radiation

Presentation for FCC and FAA Engineering Staff
by Robert A. Surette

Abstract

The FCC's adoption of rules concerning human exposure to non-ionizing RF radiation has created interest in minimizing the downward radiation generated by broadcast antennas. This bulletin presents:

- a theoretical discussion of how an array of elements produces an elevation pattern
- the effects of changing bay-to-bay spacing on downward radiation
- elevation patterns for several practical arrays, varying the number of bays and the bay-to-bay spacing (with constant amplitude and phase)
- the effects of modifying the amplitude of an array to produce a single lobe.

Document No. tb-reducing_downward_radiation (150320)

A Division of Howell Laboratories, Inc., P. O. Box 389, Bridgton, Maine 04009 USA www.shively.com
(207) 647-3327 1-888-SHIVELY Fax: (207)647-8273 sales@shively.com
An Employee-Owned Company *Certified to ISO-9001*

Introduction

Effective January 1, 1986, the FCC adopted American National Standard (ANSI) C95.1-1982, limiting human exposure to nonionizing RF radiation. In some cases, it is possible to limit human exposure by installing the broadcast antenna in an inaccessible location or by fencing off the antenna site. Such remedies are not always available or practical. Then it becomes necessary to achieve compliance with the rules by manipulating the antenna's elevation pattern to reduce downward radiation. This paper explains how antennas create downward radiation and how the intensity of downward radiation can be minimized.

Antenna array theory

Antenna arrays operate on the principle of superposition of electromagnetic (EM) fields in space; when there are more than one source of EM fields, the total field at any point in space is simply the vector sum of the fields from each source at that point in space. In theory, summing the fields at some location due to multiple sources at another location is a simple concept; however, in practice, this quickly becomes cumbersome. Antenna array theory has developed some approximations and shortcuts to make the task of determining an array's pattern easier.

The first approximation involves the distance from the array at which field intensity is to be determined. To simplify the math, only "far field" patterns are considered. In the far field, the EM fields radiated by the array can be approximated by plane waves.

The far field region is defined as anywhere in space that meets the condition:

$$R \geq 2D^2 / \lambda ,$$

as shown in figure 1, where R is the distance from the array, D is the length of the array (the physical aperture) and λ is the wavelength of the antenna. An example: For the five-bay full-wave-spaced antenna shown in figure 1, λ is about ten feet, so D is about 40 feet.

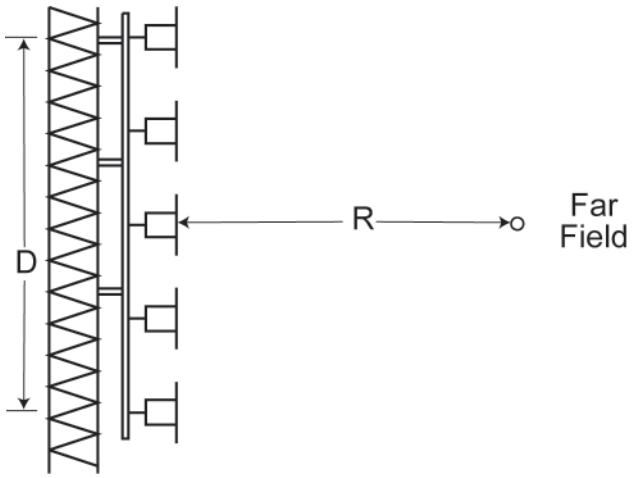

Figure 1. The Far Field Region

Then: $R \geq 2D^2 / \lambda$

or: $R \geq 2(40)^2/10$

or: $R \geq 320$ feet.

When R is less than $2D^2 / \lambda$, our simplifying assumptions become inaccurate and the calculated pattern is a poor approximation of the true pattern.

Two results of the far field assumption are our ability to use plane wave approximations, mentioned above, for the radiated fields, and the ability to separate the total array pattern into two components: one due to the characteristics of the radiators used (the "unit pattern") and the other due to the number and spacing of the radiators (the "array factor").

Plane waves propagate through space in a well known manner, the E and H fields being attenuated by 1/r and having a phase dependency of $e^{-j\beta r}$ where $\beta = 2\pi/\lambda$ and r is the radial distance from the source to the point at which the plane wave is being observed. This will be useful a bit later to determine patterns.

Antenna patterns, in the most general case, vary in three dimensions or with three variables. The most common system for describing the pattern is the spherical coordinate system, using r, the distance from the origin (usually the antenna center of radiation) to the point of observation, φ, the angular displacement of the point of observation in the x-y plane from the x axis; and θ, the angular displacement of the point of observation from the +z axis in the plane containing the point and the z axis. This is shown in figure 2.

The more familiar x, y, z coordinate system could be used (and is used as a reference for the r , φ , θ system), but would result in much more complex equations. In the case of most broadcast antenna patterns, we use a normalized pattern where the maximum field intensity is set equal to unity, and we assume an omnidirectional azimuth pattern. These two assumptions will be made here, allowing us to eliminate r and φ as variables in our pattern; thus we look only at the elevation pattern, which varies only as a function of θ. If we call the total elevation field pattern F(θ), the use of the far field approximation allows us to write this in two parts:

$$F(\theta) = A(\theta)\, E(\theta)$$

where $E(\theta)$ is the elevation pattern of a single radiator and $A(\theta)$ is the array factor - that portion of the total elevation pattern due to the spacing, number, magnitude and phase of the array elements, no matter what type radiator each element may be. Notice that if either $E(\theta) = 0$ or $A(\theta) = 0$, the total pattern, $F(\theta)$ = zero. This is where arrays are useful in controlling radiation: even if an individual radiator radiates power in an undesirable direction (such as downward), an array can often be designed to nullify that effect and eliminate radiation in that direction. Let's take a look at how this can be done.

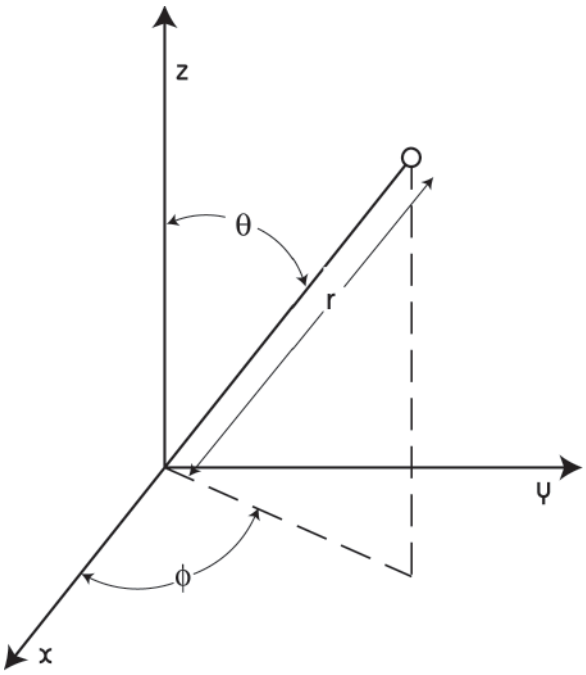

Figure 2. Spherical Coordinate System

Array factors for small arrays

For small arrays using only a few elements, a general idea of the array factor effect can be found by inspection. For now, we'll assume each radiator to be isotropic, i.e. one that radiates equally in all directions. Figure 3a shows the geometry of a two-element full-wave-spaced array. The amplitude and phase of the current fed to each radiator are equal; they are indicated on the left of each radiator as

$$I = ie^{+j0},$$

meaning unit amplitude and zero degrees phase.

A plane wave leaving the top radiator, #1, and traveling vertically toward the bottom radiator, #2, reaches #2 with a phase shift of βd radians, where d is the spacing between the two radiators, i.e. $d = \lambda$. This results in

$$\beta d = \beta\lambda = (2\pi/\lambda) * \lambda = 2\pi ,$$

which is equivalent to zero degrees. Therefore, the wavefronts from radiators #1 and #2 are in-phase and add in the vertical direction, doubling the fields that would exist from only a single bay in these directions.

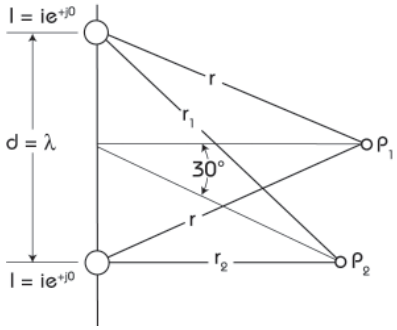

Figure 3a. Geometry, Two-Element Full-Wave-Spaced

At point P_1 , or horizontal, the plane waves leaving radiators #1 and #2 both travel the same distance, r , and therefore, both experience a phase change of βr ; since #1 and #2 started in-phase and both experienced the same phase change getting to point P_1 , they arrive at P_1 in-phase and add in the horizontal direction.

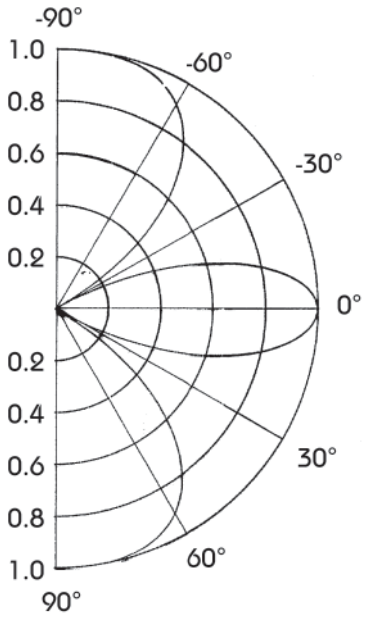

Figure 3b. Elevation Pattern, Two-Element Full-Wave-Spaced Array

At point P_2 , which is located 30° from the horizontal, a plane wave leaving #1 experiences a phase shift of βr_1 , while #2 experiences a phase shift of βr_2. Geometry shows that βr_1 and βr_2 always differ by π radians, or 180°. At 30° from the horizontal, therefore, the array has a null. More calculations at different angles would result in the pattern shown in figure 3b.

If we wish to eliminate vertical radiation in a two-element array, we have the choice of either using a radiator whose individual pattern is zero in the downward direction, or modifying the array configuration to place a null in the downward direction. Figures 4a and 4b show the same two element array as in figure 2, except that the interbay spacing has been changed to $\lambda/2$.

If we follow through an inspection as we did for figure 3 for the downward direction, we find that the plane wave radiated by #1 is shifted by

$$\beta d = \beta\lambda/2 = (2\pi/\lambda) * (\lambda/2) = \pi \text{ or } 180°$$

in getting to radiator #2. The two plane waves add out of phase to form a null in the array factor in the upward and downward directions. Further calculations result in the pattern in figure 4b for the array factor.

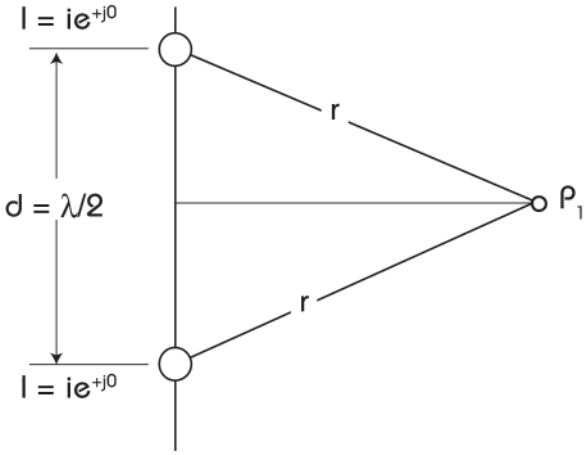

Figure 4a. Geometry, Two-Element Half-Wave-Spaced Array

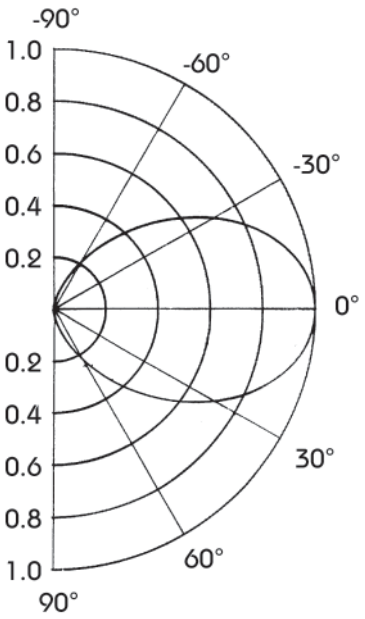

Figure 4b. Elevation Pattern, Two-Element Half-Wave-Spaced Array

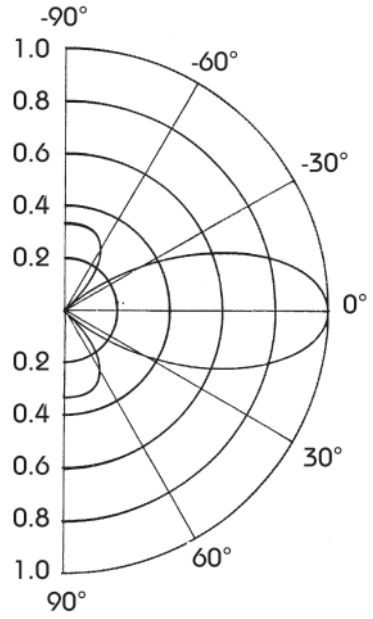

Figure 5. Three Element Half-Wavelength Spaced Array and Antenna Pattern.

Note that the array pattern has a null in the vertical directions regardless of the element pattern of the individual radiators.

The same mathematical equations can be used to calculate the pattern of a three-element half-wave-spaced array, as shown in figure 5.

The calculated array pattern shows relative field of approximately 0.3 in the vertical; i.e. at ± 90°. With an odd number of bays, the vertical radiation components from bays #1 and #2 cancel, leaving only the energy level of bay #3. And because there are three radiators, that energy level is 1/3 of the total.

Array factors for larger arrays

As previously mentioned, inspection and a little thought can often give quite a bit of insight into the general shape of the array factor of simple arrays. For more complex arrays and/or more precise pattern results, a different analysis technique is useful. This requires viewing the array as if it were a receiving array rather than a transmitting array. (Reciprocity requires that the patterns be identical in the two cases.) In the following discussion, a six element array is used as an example, but an array of any size may be treated identically.

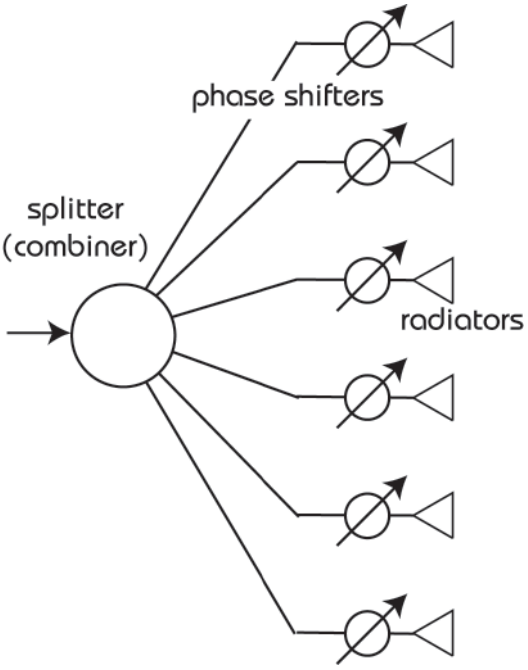

Figure 6a. Schematic, Six Element Array Feed

Figure 6 shows two schematic views of a six-element array. Figure 6a shows a six-element corporate feed such as might be used on one face of a panel antenna. The phase shifters are all set to zero and are connected to the splitter (or combiner in receiving mode) by equal lengths of line, ensuring that all the radiators are fed in-phase. In a series-fed antenna array, the same purpose is served by feeding radiators at intervals of one-wavelength, or 360 electrical degrees, along the feedline, whatever their physical physical spacing may be.

Figure 6b shows the array in the same manner as figures 2 and 3: six equally-spaced isotropic radiators in a line. The radiators are arranged symmetrically around the center of the array and are numbered -3 to +3 for convenience later on. Spacing between each two adjacent radiators is d. Also shown is a plane wave incident on the array at an angle θ. The constant phase front of the plane wave is a straight line perpendicular to the direction of propagation and shown as a dotted line. Finally, the geometry of the wavefront incident on the array is expanded for radiators #2 and #3 so that geometric relations may more easily be seen.

As seen in figure 6b, a wavefront incident on the array at an angle of θ will first encounter radiator #3. We can use this as a reference and call it "zero phase." Referring to the expanded view of radiators #2 and #3, it is easily seen that the incident wave must travel further in order to reach radiator #2 than #3.

Corresponding to this increased distance of travel is a phase lag with respect to #3 of βL = βdcosθ. The two radiators, #3 and #2, then have excitations of

$$Ie^{-j0} \text{ and } Ie^{-j\beta d\cos\theta}$$

respectively. (The amplitude of the plane wave at each radiator will be nearly identical and, without any loss in generality, can be assumed to be unity.).

Now we return to the whole six element array. A quick look shows that each element has the same relationship with the element below it as #2 had with #3; i.e. lags it by $e^{-j\beta d\cos\theta}$. This could just as easily be stated as: Each bay leads the one above it by $e^{+j\beta d\cos\theta}$. Using this convention, we can find an excitation phase for each radiator in the array, where unity amplitude is assumed.

The plane wave will cause a current in each radiator, proportional in phase to the plane wave. The current in each radiator can be written as $I_0e^{-j\theta}$, where θ is the phase of that radiator's excitation. These currents then pass through the phase shifters where an additional phase shift is added. The final current from each radiator can then be written as

$$I_0e^{-j\theta_1}e^{-j\alpha_1}$$

where θ_i is the phase solely due to the plane wave's shift at the i_{th} radiator with respect to the reference point and α_i is the phase shift due to the i_{th} phase shifter.

The currents from all radiators are then summed in the combining network. Using radiator #3 as the zero phase reference point, this summation can be written as

$$I_{total} = I_{-3} + I_{-2} + I_{-1} + I_1 + I_2 + I_3 ,$$

and substituting in the actual currents:

$$I_0[e^{-j(\theta_1 + \alpha_1)} + e^{-j(\theta_2 + \alpha_2)} + e^{-j(\theta_3 + \alpha_3)} + e^{-j(\theta_{-3} + \alpha_{-3})} + e^{-j(\theta_{-2} + \alpha_{-2})} + e^{-j(\theta_{-1} + \alpha_{-1})}] =$$

$$I_0[e^{-j(3\beta d\cos\theta + \alpha_{-1})} + e^{-j(4\beta d\cos\theta + \alpha_{-2})} + e^{-j(5\beta d\cos\theta + \alpha_{-3})} + e^{-j(0 + \alpha_3)} + e^{-j(\beta d\cos\theta + \alpha_2)} + e^{-j(2\beta d\cos\theta + \alpha_1)}]$$

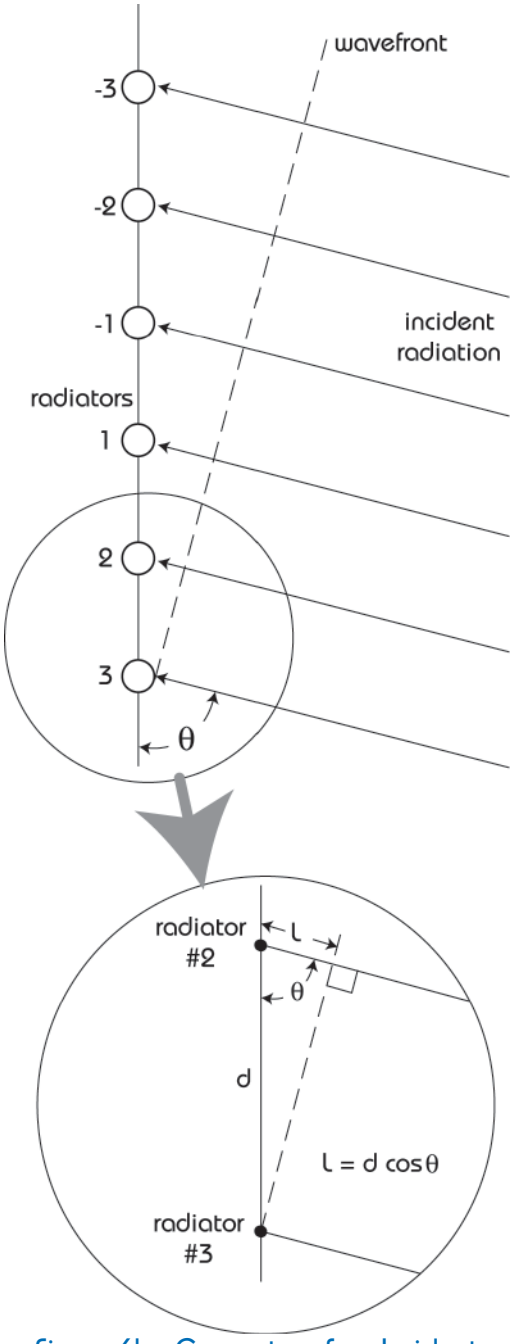

Figure 6b. Geometry of an Incident Plane Wave on a Six-Element Array

If we assume all phase shifters to be neutral, i.e. to add zero phase shift (quite common in broadcasting) then this expression becomes

$$I_{total} = I_0[e\text{-}j_0 + e^{-j\beta d\cos\theta} + e^{-2j\beta d\cos\theta} + e^{-3j\beta d\cos\theta} + e^{-4j\beta d\cos\theta} + e^{-5j\beta d\cos\theta}]$$

This expression could be plotted (as a function of θ) by taking the sum of real and imaginary parts and finding the magnitude. In many cases, this must be done; however, in this case, there are a few tricks that simplify it a bit more. If we factor out an $e^{-5j\beta d\cos\theta/2}$ and rearrange terms slightly, the result is:

$$I_{total} = I_0e^{-5j\beta d\cos\theta/2}\,[e^{-5j\beta d\cos\theta/2} + e^{+5j\beta d\cos\theta/2} + e^{-3j\beta d\cos\theta/2} + e^{+3j\beta d\cos\theta/2} + e^{-j\beta d\cos\theta/2} + e^{j\beta d\cos\theta/2}]$$

But: $e^{\pm jx} = \cos x \pm j \sin x$

So: $= 2I_0 e^{-5j\beta d\cos\theta/2} [\cos(5\beta d\cos\theta) + \cos(3\beta d\cos\theta) + \cos(\beta d\cos\theta)]$

This is the array factor.

The cosine of θ is zero when θ is an odd multiple of 90° or π/2. Looking at the array factor above, we see it is composed of terms all of which are in the form cos(nβdcosθ/2). We can use this fact to place a null in a desired location by making cos(nβdcosθ/2) go to zero at that location. In order for this to occur, nβdcosθ/2 must be an odd multiple of π/2 for the direction, θ_0 , at which we want a null. Looking at figure 6, we see that downwards (the most common direction of a desired null) is at $\theta_0 = 0°$. (Please note that this is different from the usual broadcast convention of displaying elevation patterns which use 0° as horizontal.)

If we set: $n \beta d \cos\theta / 2 = n \pi / 2$

at: $\theta = 0°$, where $\cos\theta = 1$

then: $n \beta d (1) / 2 = n \pi / 2$

or: $\beta d = \pi$ or $d = \pi / \beta$

But: $\beta = 2 \pi / \lambda$

thus: $d = \pi \lambda / 2 \pi$

Finally: $d = \lambda / 2$

The foregoing demonstrates that in a half-wave-spaced array of isotropic radiators, the relative field intensity at ± 90° from the horizontal is zero.

Figure 7 shows the array factor for a six element, one-wavelength (d = λ)-spaced array of isotropic radiators (i.e. theoretical radiators radiating equally in all directions) in polar format. Notice that the beam widths are wider at ± 90° than at 0°. Also note the levels of the side lobes at other angles (15°, 25°, 35°, 50°, etc.).

Now look at the plot in figure 8. This array is identical to that shown in figure 7 except that the spacing has been changed to half-wave. The array is now physically smaller. The number of side lobes has decreased; the width of the main lobe has increased compared to full wave spacing; and most importantly, the vertical radiation lobes have been eliminated!

Factoring in the radiator element unit pattern

Restating the definition of the total elevation field pattern equation (from page 2):

$$F(\theta) = A(\theta)\, E(\theta)$$

Up until now, we have used theoretical isotropic elements, assuming away the unit pattern of the elements [E(θ) = 1] - thus we have been able to focus on the array factor [A(θ)].

Now we need to consider the element unit pattern and its effect on the equation. In most cases, the unit pattern conforms to a cosine to the 1.5 power. The following figures use this estimate and yield results more representative of real antennas. (The calculated gains have a 4% feed system cumulative loss factor for each array, so that the values are both conservative and consistent with standard engineering practices.)

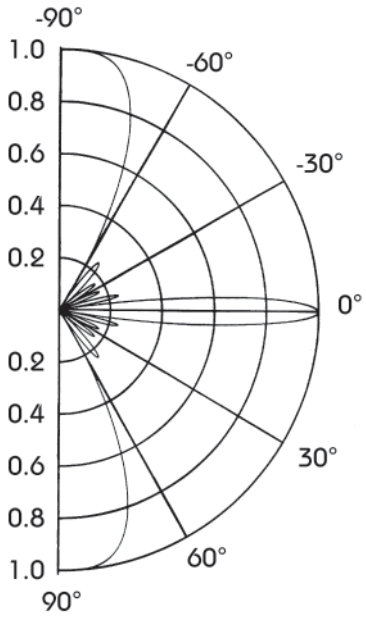

Figure 7. Field Elevation Pattern Plot, Six-Bay, Full-Wave-Spaced Array of Theoretical Isotropic Radiators

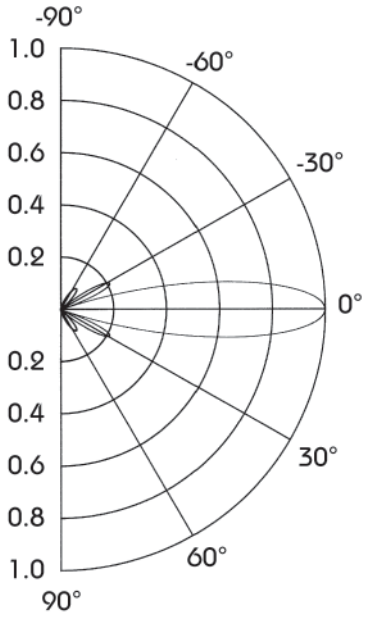

Figure 8. Field Elevation Pattern Plot, Six-Bay 1/2-Wave-Spaced Array of Theoretical Isotropic Radiators

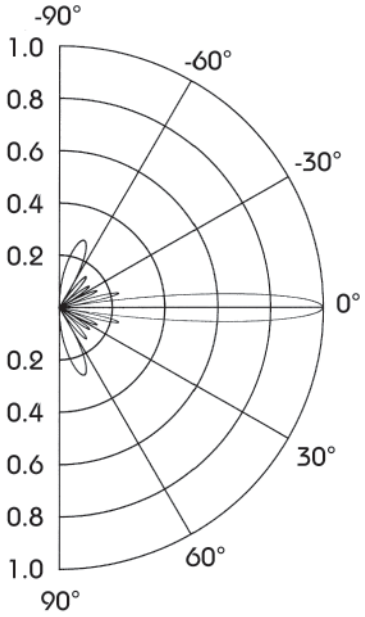

Figure 9. Field Elevation Pattern Plots, Six-Bay Full-Wave-Spaced Array Gain = 3.28

Figure 9 is the elevation pattern for a six-bay array of radiators equally spaced at one wavelength and uniformly fed. This pattern is representative of ring radiators as well as panels or stand-alone dipoles. Note that the maximum downward component is at approximately 70° depression angle, not at 90° as some people have suggested.

Some radiators have more complex unit patterns that do not follow the $\cos^{1.5}$ rule. Therefore, in reality, the amount of radiation at ±90° may not be zero.

Effect of spacing on power gain

The gain of an array can be maximized by adjusting the spacing between the radiators. Figure 10 shows an array of six bays spaced at 0.95 wavelength. Comparing figure 10 to figure 9, it will be seen that the only substantive difference is the decrease in the minor lobe at about 70°. The antenna is a little more efficient, resulting in a slight power gain increase from 3.28 to 3.31.

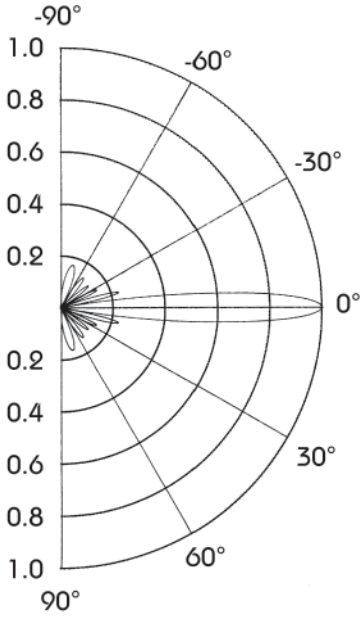

Figure 10. Field Elevation Pattern Plots, Six-Bay 0.95λ-Spaced Array Gain = 3.31

For different numbers of radiators, the spacing for maximum gain will differ. It is interesting to note that the increase in gain comes mainly from reducing the energy in the lobe at 70°, while the other side lobes are essentially unchanged.

In figure 11, the spacing has been reduced to 0.90 wavelength. The gain is now 3.22, and the side lobes are noticeably different from those in figures 9 and 10.

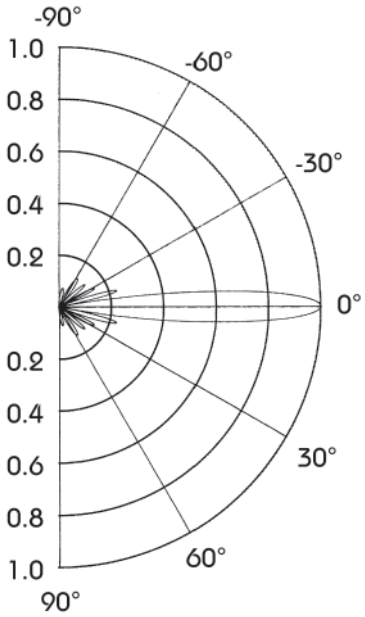

Figure 11. Field Elevation Pattern Plots, Six-Bay 0.90λ-Spaced Array Gain = 3.22

Figure 12 shows a six-bay spaced at 0.75 wavelength. The pattern is now quite different from the last three. The sixth side lobe has disappeared, and the gain is now down to 2.76.

In figure 13, the spacing has been reduced to 0.5 wavelength. This is the optimum spacing for reducing downward radiation, as shown previously. The gain is now 1.92, a reduction of 2.33 dB from that at full-wave spacing, and the total array aperture is now approximately 25 feet, down from the original 50 feet. The major lobe is now wider, and there are only two minor lobes with virtually no energy below 75° of depression angle. This is the type of pattern which may satisfy some of the new standards for downward radiation, but because of the loss in gain, more transmitter output power is needed - an expensive option - or the gain can be recovered by adding more half-wave-spaced radiators.

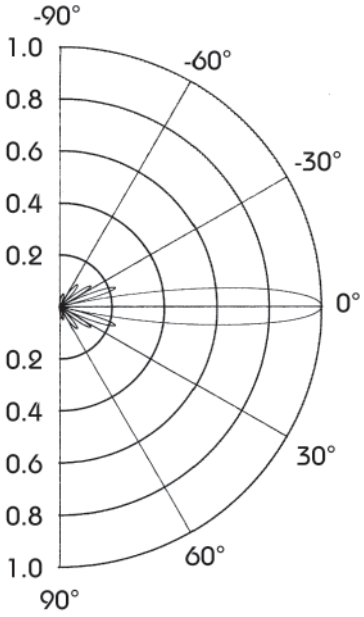

Figure 12. Field Elevation Pattern Plots, Six-Bay 0.75λ-Spaced Array Gain = 2.76

Figure 14 is the result of maintaining the same physical aperture as the original six-bay shown in figure 9 by filling the gaps between bays with five additional radiators, and creating an eleven-bay half-wave-spaced array.

The gain of this array is 3.44, which is slightly higher than the 3.28 gain of the original six-bay array.

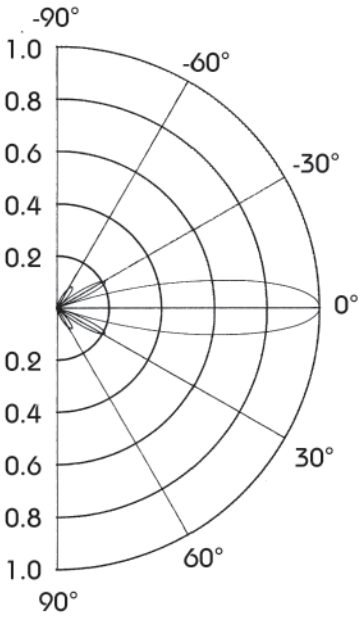

Figure 13. Field Elevation Pattern Plots, Six-Bay Half-Wave-Spaced Array Gain = 1.92

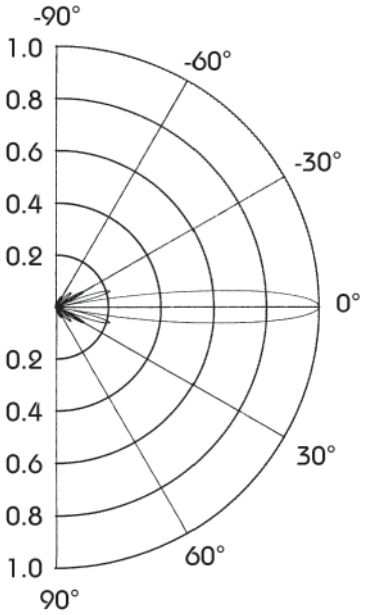

Figure 15. Field Elevation Pattern Plots, Ten-Bay Half-Wave-Spaced Array Gain = 3.14

An eleven-bay array is not a practical antenna system. A ten- or twelve-bay half-wave-spaced array would be preferred; figure 15 shows a ten-bay. Note that the ten-bay array has slightly less gain than the original six-bay array. Comparing the six-bay wavelength spaced array (figure 9) to the ten-bay half-wave-spaced array (figure 15), you will see that in this ten-bay array, radiation is dramatically suppressed beyond ±50° from the horizon - and this antenna is five feet shorter than the original 6-bay!

What we have just shown is that by changing the spacing of the elements, while maintaining constant amplitude and phase to each element, we can modify the elevation pattern to substantially reduce downward radiation.

Control of side lobes by amplitude modifications

Still using half-wave spacing, we will now manipulate the amplitude of the individual radiators to not only reduce the downward lobe, but to virtually eliminate all the side lobes, so that we end up with an antenna system that only has one main lobe.

For this comparison, we'll use a four-bay array. Compare figures 16 (full-wave-spaced) and 17 (half-wave-spaced). As above, going to half-wave-spacing eliminates the side lobe at about 70° and reduces the gain substantially.

Now we are going to reduce the amplitude of the two end bays of the same half-wave-spaced antenna shown in figure 17. The results are shown in figure 18. As you can see, the side lobe at approximately 45° in figure 17 has been almost eliminated, and the gain has been reduced to 1.15. If the amplitude of the two end bays is reduced further, the above minor lobe is totally eliminated, but the gain drops to 1.01 (figure 19). So the trade-off is between the gain of the array and the degree to which the minor lobes are reduced.

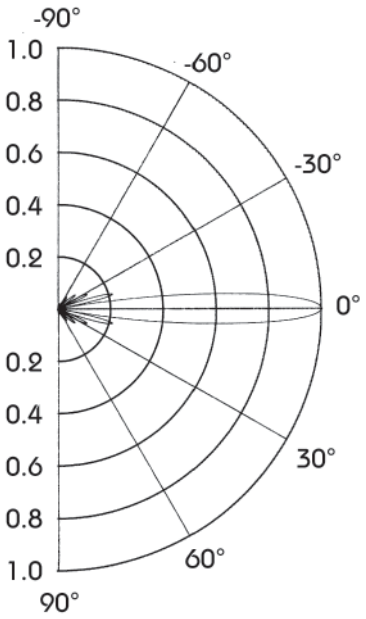

Figure 14. Field Elevation Pattern Plots, Eleven-Bay Half-Wave-Spaced Array Gain = 3.44

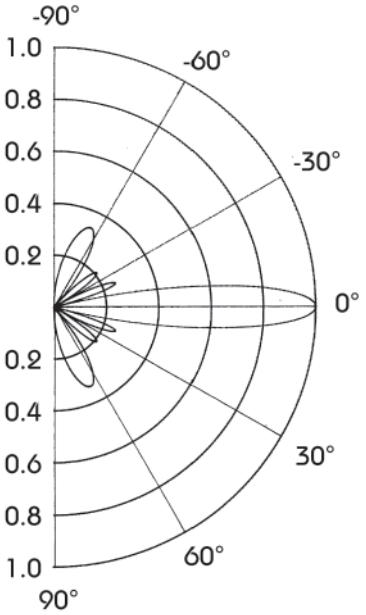

Figure 16. Field Elevation Pattern Plot, Four-Bay Full-Wave-Spaced Array Gain = 2.12

As before, we can recover the gain of the array by adding more radiators. Figures 20 and 21 show the elevation pattern of a six-bay half-wave-spaced array with reduced amplitude to the top two and bottom two radiators. Both show increased gain compared to the four-bays in figures 18 and 19.

The array in figure 21 has more amplitude reduction than the one in figure 20. Note that as with the four-bay, the additional amplitude reduction causes both further side lobe elimination and further gain loss.

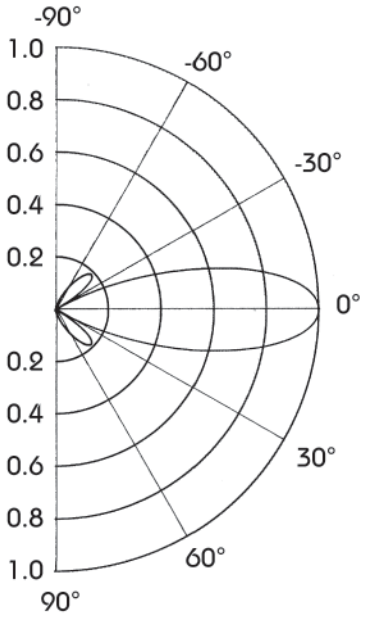

Figure 17. Field Elevation Pattern Plot, Four-Bay Half-Wave-Spaced Array
Gain = 1.31

Phase changes

We have not discussed phase changes to the individual radiators here, because changing the phase results in tilting the main lobe, better known as beam tilt, or adding null fill to the array, and is usually used for those purposes rather than eliminating downward radiation.

Conclusion

This paper has shown the basic principles of how elevation patterns are formed and how by manipulating the number of radiators and the spacing of the radiators, and changing the amplitude of the feed to the radiators, we can reduce or eliminate downward radiation.

Broadcasters are now required by the FCC to comply with tighter restrictions on levels of human exposure to RF radiation. A working knowledge of antenna array theory makes techniques available to them to allow compliance without resorting to drastic measures ...ers or moving to remote sites.

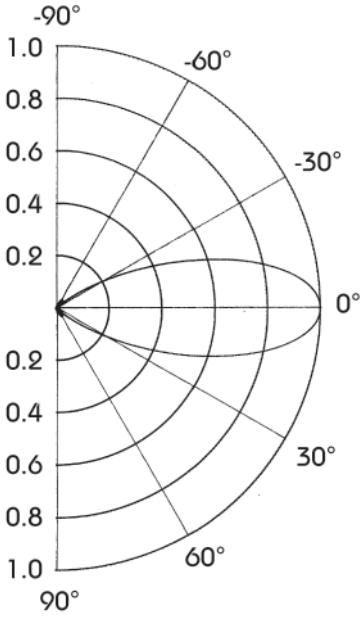

Figure 18. Field Elevation Pattern Plot, Four-Bay Half-Wave-Spaced Array with Reduced Amplitude to Outer Radiators
Gain = 1.15

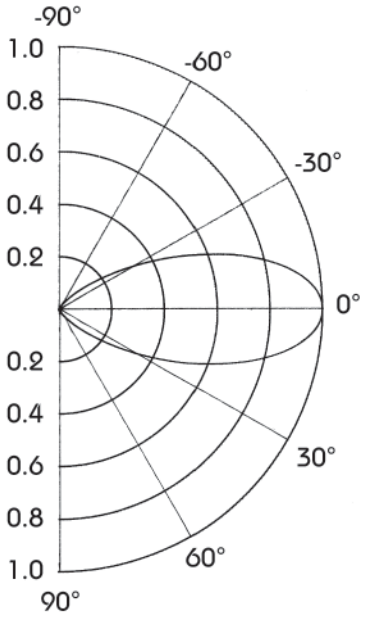

Figure 19. Field Elevation Pattern Plot, Four-Bay Half-Wave-Spaced Array with Reduced Amplitude to Outer Radiators
Gain = 1.01

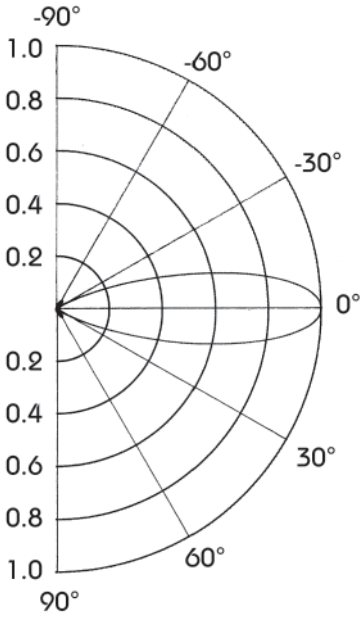

Figure 20. Field Elevation Pattern Plot, Six-Bay Half-Wave-Spaced Array
Gain = 1.56

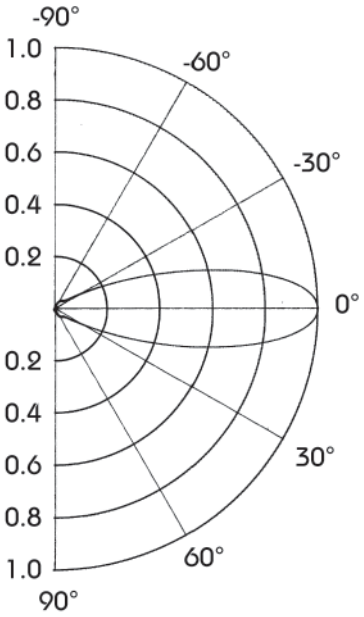

Figure 21. Field Elevation Pattern Plot, Six-Bay Half-Wave-Spaced Array
Gain = 1.41